Jurnal Kejuruteraan 38(7) 2026: 3303-3320
https://doi.org/10.17576/jkukm-2026-38(7)-11

Experimental Investigation of Heat Transfer Enhancement for CuO and Graphene Nanofluids in Corrugated Backward-Facing Step Channels with Obstacle

Taghreed Kadom Sarhan[a*], Mohd Khairol Anuar Mohd Ariffin[a*], Razi Al-Zubaidi[c], Eris Elianddy Supeni[a], Kamarul Arifin Ahmad[b] & Abd. Rahim Abu Talib[b]

[a]*Department of Mechanical Engineering, Faculty of Engineering, Universiti Putra Malaysia (UPM), 43400, Serdang, Selangor, Malaysia*

[b]*Department of Aerospace Engineering, Faculty of Engineering, Universiti Putra Malaysia (UPM), 43400, Serdang, Selangor, Malaysia*

[c]*Lincoln University College, 47301, Petaling Jaya, Selangor, Malaysia.*

[*]*Corresponding authors: tagreedkadom22@gmail.com & khairol@upm.edu.my*

Received 4 December 2025, Received in revised form 10 June 2026
Accepted 10 July 2026, Available online 30 October 2026

ABSTRACT

The friction factor and heat transfer rate of CuO-water and GO-water nanofluids on a backward-facing step (BFS) channel with trapezoidal corrugated walls and obstacle are experimentally studied by forced convection. Nanoparticles of CuO and Graphene were dispersed in water at volume concentrations of 0.1-1.0%. Tests were performed in turbulent flow in the Reynolds number range from 5000 to 20,000 at uniform heat flux of 40 kW/m². Nusselt number (Nu) increases with Re and concentration of nanoparticles. At Re = 20,000 and the concentration of 1.0% of nanofluid, the Nu of graphene-water nanofluid was 194, which is about 17% greater than that of water; meanwhile, the Nu of CuO-water nanofluid was 185 which is better than water by 12%. The friction factor also increased with nanoparticles loading and they obtained about ~35% higher and ~40% higher than water for CuO and graphene, respectively at Re = 5000. At low Re, the maximum performance evaluation criterion (PEC) of 0.5% graphene and 1% CuO was 1.74 and 1.58%, respectively, confirming the high thermal-hydraulic performance of graphene in the BFS channel.

Keywords: Backward-Facing Step (BFS); heat transfer; graphene nanofluids; CuO nanofluids experimental nusselt number

INTRODUCTION

With the rapid development of modern technological and energy systems, the need for advanced thermal management solutions has been on the rise. Traditional cooling techniques have been found to have limitations as the electronic devices become more compact, the power densities become higher and the industrial processes become more complicated. Water, ethylene glycol, and engine oil are still largely used, but due to their low thermal conductivity they do not meet the thermal requirements of high-performance systems (Ibrahim et al. 2025; Taghreed et al. 2025; Barai et al. 2023), which has been driving the search for new cooling strategies that combine high thermal transport efficiency with hydraulic stability (GaneshKumar et al. 2024; Lahmer et al. 2023).

There is great potential in the application of spray cooling (GaneshKumar et al. 2024), microchannel heat sinks (Lahmer et al. 2023), film evaporation, FEEDS-based cooling, and electrocaloric devices (Wang et al. 2024). However, their high cost, scalability problems and high levels of complexity prevent their widespread use. In contrast, nanofluids (engineered suspensions of nanosized particles (1-100 nm) in base fluids) have emerged as one of the most effective methods in the last two decades (Sohel Murshed & Nieto de Castro 2017). Due to their enhanced thermo physical properties they are of interest for several applications such as solar collectors, electronic cooling and compact heat exchangers (Chakraborty et al. 2024).

NANOFLUIDS AND THEIR THERMAL POTENTIAL

Nanoparticles enhance fluid performance through their small size, large surface area, and high intrinsic thermal conductivity (Veeranna, Sridhara & Satapathy 2011). Compared to larger additives, they improve dispersion and reduce sedimentation (Yang et al. 2020). Studies report thermal conductivity improvements of up to 49% at high particle loadings (Ahmed et al. 2023). Still, excessive concentration can raise viscosity, pressure drop, and pumping power requirements, highlighting the need for an optimal balance (Magaji, Ibrahim, Azeez & Sopian 2025; Magaji, Ibrahim, Azeez, Sopian, et al. 2025; Gupta & Subbarao 2024).

Metal oxide nanofluids such as Al_2O_3, TiO_2, NiO, and Fe_3O_4, as well as carbon-based systems like graphene and CNTs, have been extensively studied. Al_2O_3 and NiO can achieve up to 125% conductivity gains under certain conditions (Veeranna, Sridhara & Satapathy 2011), while Fe_3O_4 offers magnetically tunable thermal performance transfer (Mohammadfam & Zeinali Heris 2023). However, particle agglomeration and sedimentation remain major challenges (Veeranna, Sridhara & Satapathy 2011). Beyond heat conduction, nanofluids also enhance energy and momentum transfer while reducing erosion compared to larger suspended solids (Devendiran & Amirtham 2016).

CUO AND GRAPHENE NANOFLUIDS

CuO and graphene appear to be promising as they are cheap and have good thermophysical properties. CuO nanofluids have been reported a thermal conductivity and Nusselt number enhancements for several systems. Improvements have been reported in *Nu* by 18-35% for helically coiled tubes (Korpyś et al. 2020), in the conductivity and heat transfer coefficients in compact exchangers from 13-31% (Kiaee et al. 2020), and in the efficiency of solar collectors of 4.27% (Belkassmi et al. 2021). They are fairly easy to prepare by two-step synthesis and improved stability can be achieved by surfactants (Fazeli et al. 2021) It has been also demonstrated that nanofluids made of CNTs and nano-silica can enhance the material performance in quenching applications (Mubasyir, M. M. et al. 2021).

Graphene nanoplatelets (GNPs) and GO have extremely high in-plane conductivity (3000-5000 W/m.K), much higher than metal oxides (Shaik et al. 2024; Siow et al. 2024). Graphene-based nanocomposites have also been found to possess enhanced thermal conductivity, which is also indicative of graphene's potential use for thermal management applications (Othman, Raja N. & Zainordin 2021). They offer excellent convective heat transfer with minimal viscosity increase and therewith low pumping requirements (Ozturk et al. 2013). For example, 0.06 wt.% GNP in water increased convective heat transfer in shell-and-tube exchangers by 22.47% (Zolfalizadeh et al. 2023), in smooth tubes with inserts, PEC values as high as 2.5 were achieved at 1% concentration (Dagdelen & Ozceyhan 2024). Graphene nanofluids have also been shown to exhibit good suspension stability (Zolfalizadeh et al. 2023), wettability enhancement and stable conductivity under changes in thermal and pressure conditions (Guo et al. 2024; Ren et al. 2024).

Comparison between different nanofluids shows that CuO nanofluids are unstable, prone to aggregation at higher loadings (Salameh et al. 2023) while graphene nanofluids especially with surface modifications are more stable and conductive at higher levels (Azizi & Honarvar 2021; Komeilibirjandi et al. 2020). Agglomeration may be a drawback to dispersion and performance of nanoparticles, particularly at higher thermal treatment conditions or when not adequately supported with a surfactant (Samad et al. 2018). Graphene is suitable for tubular exchangers and complex flows (Dagdelen & Ozceyhan 2024) while CuO is used for cooling of building and microchannel exchanger (Syed 2025; Thangapandian & Palanisamy 2022).

PERFORMANCE INDICATORS AND SYSTEM-LEVEL BEHAVIOR

Among the several influencing factors, nanoparticle concentration, flow regime, and geometry are the most important parameters that determine heat transfer efficiency which is denoted by Nusselt number (*Nu*). *Nu* is intensified by the CuO nanofluids, as it influences conductivity and Brownian motion (Wang et al. 2022; Rahimi et al. 2018), and is higher with high stability for the graphene nanofluids (Syed 2025; Shaik et al. 2024). Improving the *Nu* tends to increase the flow resistance, a design trade-off. Twisted tubes, variable cross section microchannels, and porous media are among the modifications that can strongly enhance *Nu* at the cost of increasing pressure drops (Yanlin et al. 2024; Ming et al. 2010). Thus, the geometry and surface treatments optimization is a key factor in the maintenance of efficiency (Wang et al. 2024; Huang & Pan 2021).

Applications are becoming increasingly promising: graphene nanofluids have been applied to electronic cooling, green refrigerants and heat exchangers (Ishii et al. 2024), while CuO nanofluids are common in HVAC and compact exchangers (Xu et al. 2025). Hybrid Cu-graphene nanofluids are more stable and provide better

thermal performance than the former and the latter separately (Shaik et al. 2024).

Concentration effects are significant: at low loadings (0.1-0.5%) stability and flow homogeneity is improved while at high loadings (0.5-1.0%) turbulence and *Nu* are increased at the expense of pressure penalties (Abdulrazzaq et al. 2020; Rahimi Gheynani et al. 2019). In the mixed convection in porous cavities and lid driven cavity (Asadi et al. 2020) CuO is used to improve heat transfer, and in the mixed convection with inserts, graphene nanofluids are used to provide better exchanger performance (Syed 2025).

NANOPARTICLE CONCENTRATION, SIZE, AND HYBRID EFFECTS

The concentration of nanoparticles plays an important role in nanofluid research. Even very low loadings (0.1 wt.% graphene oxide) have been proven to reach values of 0.380 W/mK (Khouri et al. 2024), and a 26.2% conductivity enhancement has been obtained for 0.1 vol.% ZrO2/EG (Barai et al. 2023). Metal oxide and carbon system hybrids have been found to be synergistic in nature and Al2O3-ZnO-MWCNT/EG nanofluids show 26.6% improvement at a concentration as low as 0.05% (Bindu & Joselin Herbert 2022). Further, the Cu-graphene hybrid nanofluids have shown ~35% conductivity and good stability (Shaik et al. 2024).

Particle size is also a key factor when it comes to nanofluid behavior. Surface area and Brownian motion are greater for small particles, and as a result, small particles can provide larger convective coefficients and thermal conductivity than large particles (Heidarshenas et al. 2020). The SiO2 nanofluids have also shown a significant enhancement of the conductivity and critical heat flux for the smaller particle sizes (Milyani et al. 2023). The effect of particle morphology has also been investigated, where spherical particles are shown to have a better performance in pulsating flows and cylindrical particles in steady flows (Chamkha & Selimefendigil 2018).

NANOFLUIDS IN BACKWARD-FACING STEP (BFS) GEOMETRIES

Backward-facing step (BFS) channels offer a convenient geometry for investigating flow separation, recirculation and reattachment, which are all of direct relevance for heat transfer. Numerous studies validate the promising role of nanofluids in such systems: β-Ga_2O/water nanofluids increased *Nu* at the expense of increased pumping power (Abu Talib & Salman 2023); Al_2O_3–water nanofluids in combination with ribs and dimples enhanced the mixing and secondary vortices (Yousefi et al. 2023); hybrid Al_2O_3–Cu nanofluids under magnetic fields decreased reattachment length while increasing *Nu* (Mehrez & El Cafsi 2019). More recently, trapezoidal corrugated walls and well-designed obstacles have been experimentally investigated to show that they offer turbulence promotion and enhanced heat transfer with modest friction penalties (Taghreed et al. 2025).

However, the majority of studies on BFS are still numerical or only involve one type of nanofluid systems. Despite the fact that many experimental and numerical studies have been reported showing that SiO_2 and Al_2O_3 nanofluids can achieve a higher value of Nusselt number with tolerable frictional losses (Kherbeet et al. 2014, 2015), the study of direct experimental comparison between CuO-water and graphene-water nanofluids in BFS geometries is very limited. The experimental study of the performance of both the nanofluids under similar operating conditions in trapezoidal corrugated BFS channel with obstacle is yet to be found in particular. The previous literature is inadequate to explain their comparative performance on the Nusselt number, friction factor and overall thermal-hydraulic performance using PEC. Hence, a systematic experimental study on this gap is required to explore the potential of advanced BFS geometry, disturbance in flow caused by the obstacle and high performance nanofluids to find the optimal type and concentration of nanofluids for the compact thermal management applications (Verma et al. 2025; Massey et al. 2019).

This gap calls for systematic research that combines state-of-the-art geometries with high-performance nanofluids.

MOTIVATION AND RESEARCH OBJECTIVES

From the literature reviewed, two things become clear:

1. CuO-water and graphene-water nanofluids are among the most promising fluids for thermal management applications owing to their excellent conductivity and stability.
2. BFS geometries (especially trapezoidal corrugations and obstacles) offer great potential to further enhance the heat transfer through the intensification of recirculation and turbulence (Taghreed et al. 2025).

However, a direct, systematic comparison of CuO and graphene nanofluids under such conditions has not been

provided in any experimental study yet. An insightful comparison of their relative performance in terms of Nusselt number variation, velocity distribution, recirculation behavior and overall thermal - hydraulic efficiency is essential to guide their application in real heat exchangers and advanced cooling systems.

Therefore, in present study, the thermal and flow properties of CuO-water and graphene-water nanofluids are experimentally studied in BFS channel with trapezoidal corrugated walls with obstacle. Semi-logarithmic contours between 0.1% and 1.0% are studied over a Reynolds number range of 5000-20,000. The research focuses on:

1. Thermophysical properties of CuO and graphene nanofluids: comparison, measurement and analysis
2. Determination of variation of Nusselt number and trends of friction factor.
3. In terms of the PEC (performance evaluation criterion), a sensitivity study is performed to balance the heat transfer and hydraulic penalties.
4. Optimization for BFS-based thermal management applications: identification of the optimum nanoparticle type and concentration.

By covering this identified research gap, this work provides new experimental evidence on the comparative behavior of CuO and graphene-based nanofluids in complex geometries. The experimental results will offer helpful information for the design of new generation heat exchangers; electronic cooling devices and industrial systems where compact and efficient thermal management solutions are needed.

METHODOLOGY

EXPERIMENTAL SETUP AND APPARATUS DETAILS

The present work was conceived as a fully experimental investigation; no new numerical simulation was performed in this study and the available simulation results in the literature were only used for the validation of the experimental set up.

The experimental study was conducted in a backward-facing step (BFS) channel with trapezoidal corrugated walls and one obstacle for Model B of the proposed geometries (Taghreed et al. 2025) where the test section was made of high-purity acrylic for structural strength and optical transparency and bottom wall was made of high-purity aluminium for heat conductivity and machinability. In order to minimize thermal losses, the whole section was covered externally by fiberglass. The design of the setup is shown in Figure 1(a).

The channel dimensions were specified with inlet height h = 10 mm and outlet height H = 20 mm which provides an expansion ratio of 2. Fixed width = 50 mm with upstream L1 = 200 mm and downstream L2 = 200 mm and L3 = 100 mm for a total channel length of 500 mm. The corrugated bottom wall was designed with a trapezoidal corrugation with corrugation height a = 4 mm, pitch P = 20 mm and spacing S = 10 mm. An additional flow disturbance and, consequently, recirculation were created by an additional obstacle in the form of a rectangular plate with a length of 5 mm and placed at 90deg situated on the upper wall, at a distance 215 mm from the inlet. The complete geometric structure of the BFS test channel is presented in Figure 1(c).

This design was chosen after the previous results that showed the trapezoidal corrugated BFS with a corrugation height of 4 mm, pitch 20 mm with an obstacle of 5 mm at 215 mm provided better thermal transfer performance and higher PEC than other models with good compromise between thermal enhancement and frictional losses (Taghreed et al. 2025; Hilo et al. 2020).

A flat electrical heater plate was placed along one of the walls of the aluminum bottom of the test section in order to impose a uniform heat flux. In all the experimental runs the heated bottom wall had a constant heat flux of 40 kW/m², and the other external wall surfaces were insulated to minimize heat loss and provide controlled thermal boundary conditions. The maximum heat load of the plate was 350 W and the impinged heat flux was fixed as 40 kW/m². Power to the heater was supplied by a DC power supply with a voltage regulator to make fine control of the current and voltage inputs. In order to monitor and record the input power, a calibrated digital multimeter (BK PRECISION, 2831E) with an accuracy of ±0.03% DC voltage was added to the circuit. The actual laboratory with instrumentation, power supply and chiller connections are shown in Figure 1(b).

Distilled water, CuO-water nanofluid, and graphene-water nanofluid were used as the working fluid and circulated in the closed-loop configuration. An industrial water chiller (SPH20N) was used to regulate the inlet fluid temperature to 25 ± 0.2 °C. The chiller consisted of cooling coil, compressor and 8 L storage reservoir with a cooling capacity of 2400 kcal/h. A 0.5 Hp pump was used to provide circulation with a constant flow pattern throughout the channel. The cooling loop was used to return the fluid temperature to ambient before it re-enters the test section to achieve repeatable experimental conditions.

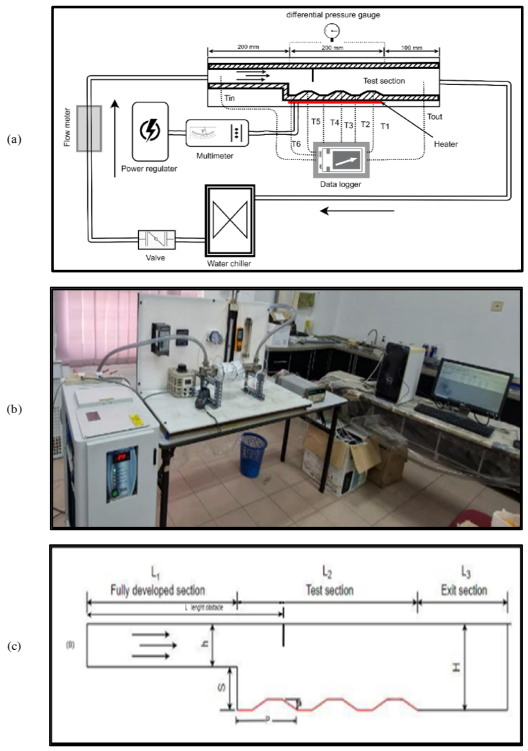


FIGURE 1. Experimental setup: (a) schematic layout, (b) laboratory arrangement, (c) test channel configuration, (d) BFS model with trapezoidal corrugated wall and obstacle

To quantify the volumetric flow rate, a flow meter with a measurement range of 4–50 LPM and accuracy of ±0.5% (FC SD70-R50, TOFCO) was placed upstream of the test section. Flow was controlled by valves found inside the chiller loop. Pressure drops across the BFS channel was measured by means of a differential pressure gauge connected to both the inlet and outlet sections of the test section.

Temperature measurement was obtained by means of eight K-type thermocouples placed along the test channel. Two thermocouples were placed at the inlet and outlet to measure the bulk fluid temperatures, and six were placed in holes drilled through the heater plate and downstream wall (less than 1 mm in diameter) and sealed with thermal epoxy. These were made with direct contact with the working fluid in order to provide accurate measurement. Figure1 (d) shows close-up view of the BFS test section with a trapezoidal aluminum wall, obstacle, thermocouples, heater and sensor locations. All thermocouples were interfaced to a multi-channel data logger (SIMEX, CMC-99 MultiCon) to record wall and fluid temperatures as a function of time. The data was only recorded when the steady state conditions were obtained and the cases were repeated to increase the reliability of measurement and to decrease the random experimental error.

PREPARATION OF NANOFLUIDS

Nanofluids were prepared by the two-step method, which is well known to provide reproducible fluids suitable for metal-oxide and carbon-based nanoparticles. Distilled water was used as the base fluid.

In this study, CuO-water nanofluids were prepared by using nanoparticles with an average particle size of 45 nm with a density of 6000 kg/m³. From the SEM image of CuO nanoparticles as shown in Figure 2(a), they are found to be aggregated and irregular in morphology. Two-step precipitation technique was adopted and precise weighing of nanoparticles was carried out in analytical balance ((±0.1 mg) followed by dispersion in distilled water. The solution was magnetically stirred for 30 min, followed by ultrasonic homogenization for 1 h (Power Sonic 410) to ensure the homogeneous dispersion and reduced agglomeration of the ink.

Graphene nanoplatelets (with thickness 60-80 nm, with density 2250 kg/m³) were employed for preparation of graphene nanofluids in distilled water. The sheet-like structure of graphene, as shown in Figure 2(b) SEM image, offers a superior in-plane thermal conductivity and stability with respect to spherical particles. The same two-step synthesis procedure was used: magnetic stirring and then one-hour ultrasonication. No surfactant has been added to prevent chemical modification of thermophysical properties. Volume concentrations in the range of 0.1-1.0% were examined. Both of the nanofluids were freshly prepared before each experimental run to ensure their stability.

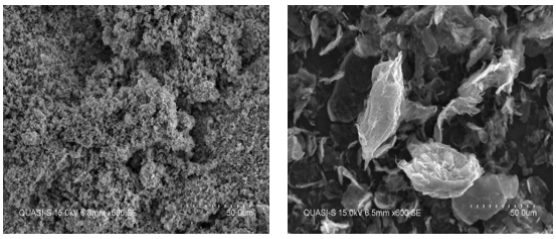


FIGURE 2. SEM Image of (a) CuO Nanoparticles (b) Graphene Nanoparticles

Nanofluids were synthesized at volume fractions of 0.1%, 0.2%, 0.3%, 0.4%, 0.5% and 1.0% as given in Table 1. These concentrations were selected to achieve good stability while providing measurable thermal improvements while avoiding excessive viscosity increase. The preparation procedure is shown in Figure 3, where (a) the ultrasonic bath helped to break the nanoparticle agglomerates, (b) the ultrasonic probe gave more depth of dispersion for homogeneous distribution, and (c) the

mechanical stirrer maintained a constant mixing in the fluid. Finally (d), the prepared nanofluid samples at different concentrations showed stable suspensions which could be used for the subsequent test experiments.

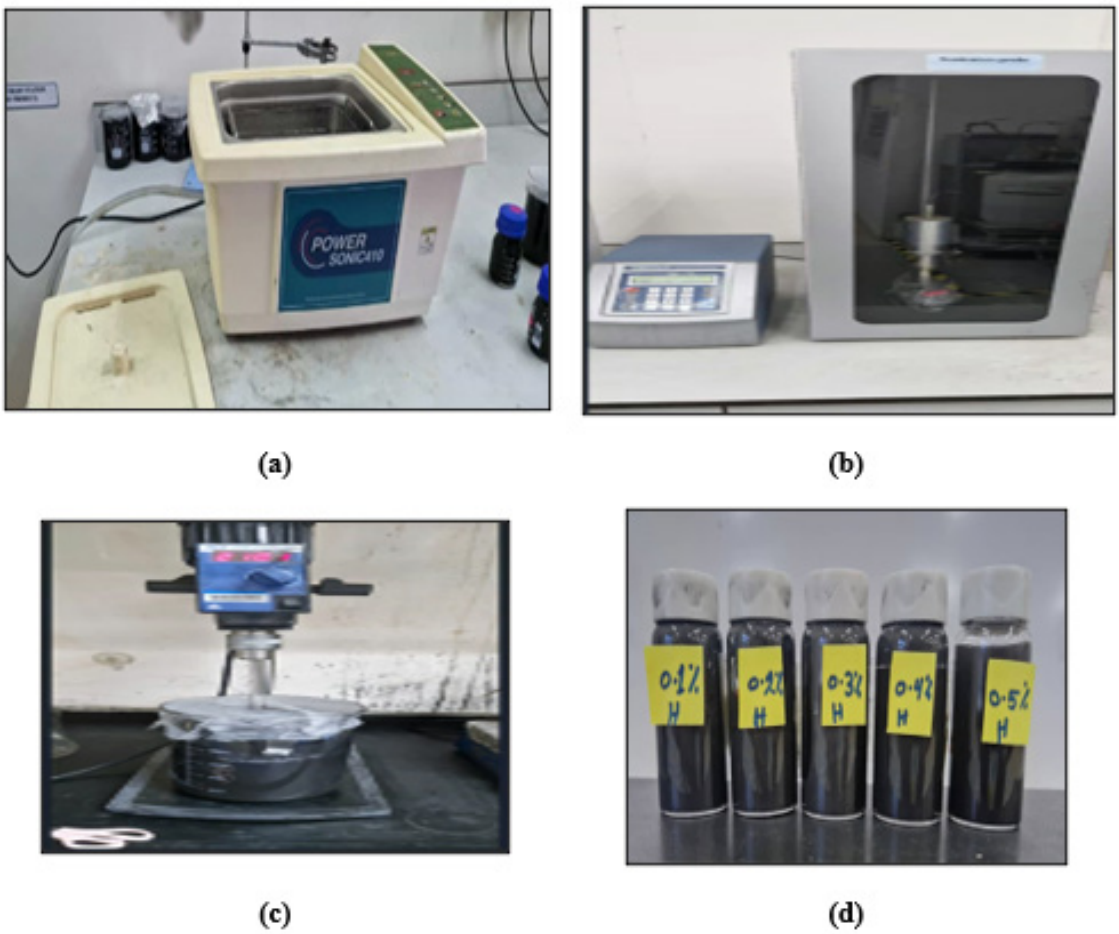


FIGURE 2. Preparation of CuO and Graphene nanofluids: (a) Ultrasonic bath, (b) Ultrasonic probe, (c) Mechanical stirrer, (d) Samples at 0.1–0.5% concentrations

TABLE 1. Weight of Nanoparticles and Volume Concentration

Volume concentration in 1 Liter of Water	CuO nanoparticles weight (***g***)	Graphene nanoparticles weight (***g***)
0.1%	6	2.3
0.2%	12	4.6
0.3%	18	6.8
0.4%	24	9.1
0.5%	30	11.4
1%	60	22.8

MEASUREMENT OF THERMOPHYSICAL PROPERTIES OF NANOFLUIDS

Before performing the heat transfer tests, thermophysical properties of the working fluids distilled water, CuO - water nanofluid, and graphene - water nanofluid were experimentally obtained. Nanofluids were made with volume concentrations of 0.1%-1.0%.

The density of the nanofluids was measured by digital density meter (DMA 1001). The viscosity was measured with a rotational viscometer (BIOBASE BDV-8S), with an accuracy of ±0.1%, while the rotational speed was controlled within the operating range to ensure the accuracy of the measurement. To provide temperature control for the fluids under test a refrigerated water bath was used.

The thermal conductivity was measured by KD2 Pro thermal property analyzer by transient hot-wire method. The instrument is accurate to within ±5% over the 0.2–2 W/m·K range for nanofluid testing. The specific heat capacity was determined by differential scanning calorimeter (DSC) in the temperature range of 40–450 °C ±2%.

For all nanofluid concentrations, each measurement was repeated five times to reduce random error and increase correct measurement reliability. Time-averaged results were then computed and used in further data analysis. The results of the measured thermophysical properties are summarized in Tables 2 to Table 4 (Ismael 2013).

TABLE 2. Thermophysical Properties of Water and Nanoparticle

Thermophysical Properties	Distill water	CuO	Graphene
Density, ρ (kg/m³)	998.203	6000	2250
Thermal conductivity, k (W/m.K)	6.13E-01	75	2000
Specific heat, cp (J/kg.K)	4182.2	535.6	710
Viscosity ($Pa\ s$)	1.01E-03	-	-

TABLE3. Thermophysical Properties of CuO Nanofluid

Properties	0.1%	0.2%	0.3%	0.4%	0.5%	1%
Density (kg/m^3)	987.8	990.7	992.6	993.0	999.8	1008.7
Viscosity ($Pa\ s$)	0.00101	0.00101	0.00101	0.00101	0.00102	0.00102
Thermal conductivity ($W/m\ k$)	0.58082	0.58852	0.59016	0.59145	0.59856	0.60230
Specific heat ($J/kg\ K$)	4074.1	4070.5	4067.0	4062.8	4059.9	3975.9

TABLE4. Thermophysical Properties of Graphene Nanofluid

Properties	0.1%	0.2%	0.3%	0.4%	0.5%	1%
Density (kg/m^3)	958.1	976.7	977.3	980.5	985.3	989.0
Viscosity ($Pa\ s$)	0.00101	0.00101	0.00101	0.00101	0.00101	0.00102
Thermal conductivity ($W/m\ k$)	0.58973	0.59153	0.59204	0.59209	0.59578	0.60051
Specific heat ($J/kg\ K$)	4074.3	4070.9	4067.5	4064.5	4060.7	3976.6

DATA REDUCTION AND UNCERTAINTY ANALYSIS

Distilled water, CuO-water and graphene-water nanofluids (at 1% volume concentration) were used to compare turbulent convection, heat transfer and frictional behavior of nanofluids flowing through backward facing step (BFS) channel. It was assumed that the inlet velocity depends on the channel hydraulic diameter and all the thermohydraulic parameters were derived from the governing equations. The inlet velocity uin is determined by the channel hydraulic diameter, the friction factor and the heat transfer is given by:

$$u_{in} = \frac{Re\, u}{\rho Dh} \tag{1}$$

The hydraulic diameter of the channel was determined from its cross-section geometry:

$$D_h = \frac{4A}{P} \tag{2}$$

The average Nusselt number which corresponds to convective heat transfer was calculated as:

$$Nu = \frac{hD_h}{k} \tag{3}$$

where D_h is the channel hydraulic diameter, A is the channel cross-section area, P is the channel wetted perimeter and A is the channel cross-section area.

Friction Factor

The pressure loss across the channel, ΔP is calculated by the following equations of Li et al. (2007), where $uave$ is

the average velocity, $\Delta Pin,out$ is inlet and outlet pressure, Pd total -loss of pressure and f is the friction factor.

$$\Delta_P = \Delta P_{in,Out} - Pd \tag{4}$$

$$Pd = 1.18\rho u_{ave}^2 \tag{5}$$

$$u_{ave} = \frac{m_i}{\rho Ac} \tag{6}$$

$$Re = \frac{u_{ave} \cdot D_h}{v} \tag{7}$$

$$f = \frac{2D_h\Delta_P}{L\rho u^2} \tag{8}$$

Where $uave$ is the average velocity, $\Delta Pin,out$ is inlet and outlet pressure, Pd total pressure loss and f is the friction factor.

Heat Transfer Calculations

The power requirement to the heater can be derived from the following equations for Ahmed et al. (2015), and Li et al. (2007):

$$\Phi = U \cdot I \tag{9}$$

$$Q = m^* C_p \Delta T \tag{10}$$

$$q = \frac{Q}{Aw} \tag{11}$$

where Φ (W) is the power supplied by the electrical DC power; q (W/m^2) is the heat flux incident on the downstream wall; and Q (W) is the heat transfer rate. The local heat transfer coefficient hx and the Nusselt number *Nu* are given by the equations of Duda (2023):

$$h_x = \frac{qL_x / L}{\Delta Tx} \; q = \frac{Q}{Aw} \tag{12}$$

$$Nu_x = \frac{h_{xD_h}}{k} = \frac{qL_x / L \cdot D_h}{\Delta Tx \cdot k} = \frac{mC_P\Delta T \cdot L_x / L \cdot D_h}{A_w \cdot \Delta Tx \cdot k} \tag{13}$$

$$h_{av} = \frac{m_{Cp}\Delta T}{A_w(T_{w\cdot av} - T_{b\cdot av})} \tag{14}$$

$$N_{uav} = \frac{h_{av}D_h}{k} \tag{15}$$

$$\Delta Tx = T_{Wx} - T_{h\cdot x\cdot in} \tag{16}$$

$$T_{b,x,in} = T_{in}\frac{q \cdot L_x / L}{\dot{m}cp} \tag{17}$$

ΔTx is the bulk temperature along the X-direction (K). Twx wall temperature along X- direction (K).

UNCERTAINTY ANALYSIS

Experimental results are only valid if the measuring devices are precise and data is acquired with the correct degree of accuracy. Each instrument has natural limitations, and all instruments are subject to both systematic and random errors. Following the approach of Mohammed & Salman (2007), uncertainties of the derived parameters including Reynolds number, Nusselt number and friction factor were estimated by error propagation:

$$R = R(X_1, X_2, \cdots, X_n) \tag{18}$$

where *R* is a dependent parameter, while *X*1, *X*2, and Xn are independent parameters. Therefore, the uncertainty of R can be calculated as follows:

$$w_R = \pm\sqrt{\left(\frac{\partial R}{\partial x}w_{x_1}\right)^2 + \left(\frac{\partial R}{\partial x_2}w_{x_2}\right)^2 + \cdots + \left(\frac{\partial R}{\partial x_i}w_{x_i}\right)} \tag{19}$$

where WXi is the uncertainty of parameter Xi.

The estimated uncertainties were 4.5% for velocity, 11.7% for the Nusselt number and 12.5% for the friction factor as shown in Table 5. High precision sensors and repeated measurements have reduced errors, but homogeneous dispersion of nanofluids is assumed ignoring particle slip, aggregation or migration. One of the implications of this work is that future work should combine multiphase models and sensor-response effects for a more accurate representation. The numerical procedures follow in Table 5.

TABLE 3. Measurement Uncertainty

No.	Variable	Uncertainty %
1	Inlet height, h	±0.1
2	Outlet height, H	±0.1
3	Width, W	±0.1
4	Length, L	±0.1
5	Inlet bulk temperature,	±0.2ºC
6	Outlet bulk temperature,	±0.2ºC

continue...

...cont.

No.	Variable	Uncertainty %
7	Wall temperature T_w	±0.2ºC
8	Thermal conductivity	±5
9	Velocity	4.5
10	Nusselt number	6.6
11	Friction factor	7.3

PERFORMANCE EVALUATION CRITERIA

Heat transfer gain was compared with frictional penalties by the performance evaluation criterion (PEC). The PEC value is greater than one when the thermal enhancement is more important than the flow resistance, which is calculated in terms of the ratio of the Nusselt number and friction factor (Manca et al. 2012). For all the numerical cases, the PEC was determined according to Eq. (20).

$$PEC = \frac{(Nu / Nu_o)}{(f / f_o)^{1/3}} \quad (20)$$

where Nu and f is the Nusselt number and the friction factor of the original case, while Nu_o and f_o is the Nusselt number and friction factor for the proposed case.

RESULTS AND DISCUSSION

The present study did not generate CFD data for comparison, but rather used the data generated by Taghreed et al. (2025) for the same trapezoidal corrugated BFS channel with an obstacle. To confirm the validity of the present experimental setup, the average Nusselt number (Nu) was compared with CFD results of trapezoidal BFS channels with an obstacle reported by (Taghreed et al. 2025). As illustrated in Figure 4, the trends of the experimental results and the numerical ones are in agreement with an average deviation of 6.5%, validating the reliability of the experimental setup (Mayo et al. 2018; Manca et al. 2012).

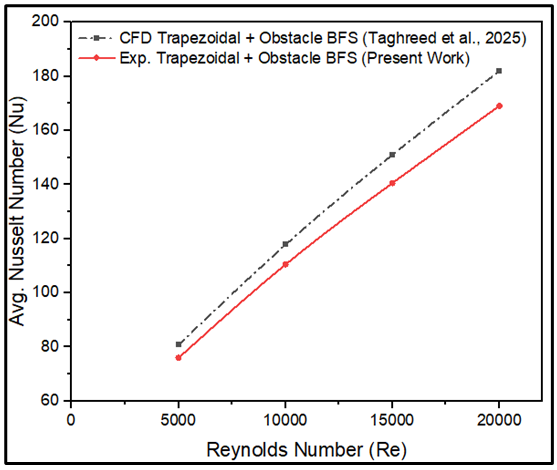


FIGURE 4. Average Nusselt number comparison between CFD and experimental results for trapezoidal BFS with obstacle

HEAT TRANSFER

Figure 5 shows the experimental results of average Nusselt number (Nu) of CuO-water nanofluids for different volume fraction and Reynolds number. As it shown in Figure 5(a), *Nu* increases with Reynolds number and nanoparticle concentration. At *Re* = 5000, the CuO nanofluid with 1% volume fraction shows an improvement of almost 12% with respect to pure water. This enhancement is more significant at higher Reynolds numbers and approaches 190.1 at *Re* = 20,000 in case of 1% CuO, while the pure water is 169. The increase is explained based on enhanced thermal conductivity and enhanced turbulence near the wall region. However, at extremely low concentrations (0.1%) the enhancement is small, which would indicate that the viscosity effects offset the thermal benefits at low loadings.

Figure 5(b) shows the change of *Nu* for graphene-water nanofluids for the same conditions. Graphene nanofluids perform better than the CuO nanofluids for the same concentration because graphene has a naturally higher thermal conductivity. When the concentration is 1%, the *Nu* is 198.3 at *Re* = 20,000, and it indicates an improvement of 17.3% compared with pure water. Significant improvements are obtained at moderate concentrations (0.3-0.5%) confirming the potential of graphene nanofluids for better heat transfer augmentation.

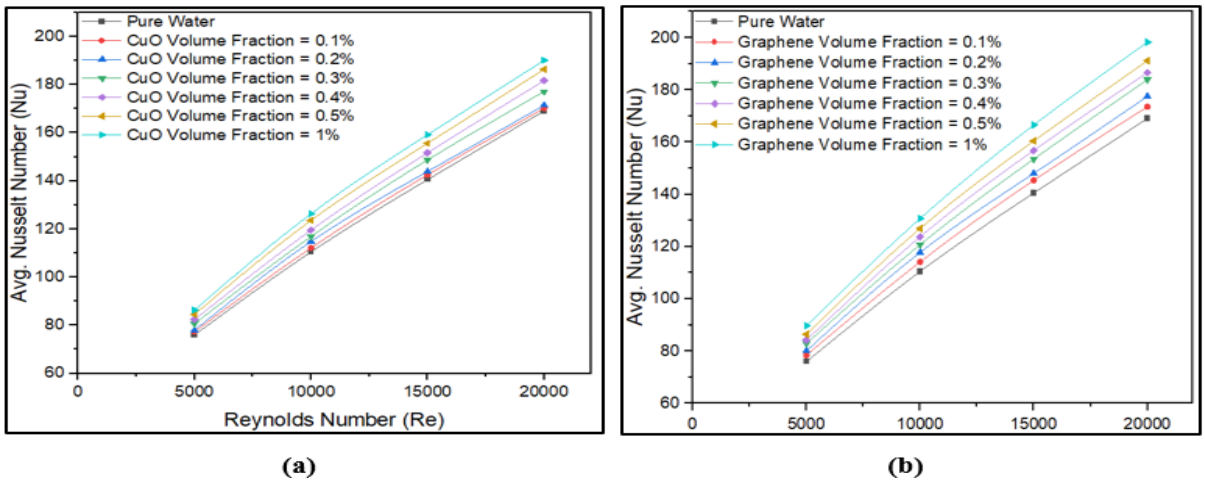


FIGURE 5. Variation of average Nusselt number (Nu) with Reynolds number (Re): (a) CuO–water nanofluids at different volume fractions (0.1–1.0%), (b) Graphene–water nanofluids at different volume fractions (0.1–1.0%).

Figure 6 shows the direct comparison of CuO and graphene nanofluids at the concentrations of 0.5% and 1%. The *Nu* values of graphene are always greater than CuO for all Reynolds number values, and the difference is more distinct for higher flow rates. For instance, at *Re* = 20,000, the graphene of 1% reaches almost 198 compared with 190 for CuO. This result suggests that graphene nanofluids are better for improving the convective heat transfer properties, especially in turbulent regimes, while CuO nanofluids exhibit a moderate but a stable behavior. These results verify the contribution of both nanofluids in enhancing the heat transfer of BFS channel, and graphene has the maximum potential for high-performance thermal management applications.

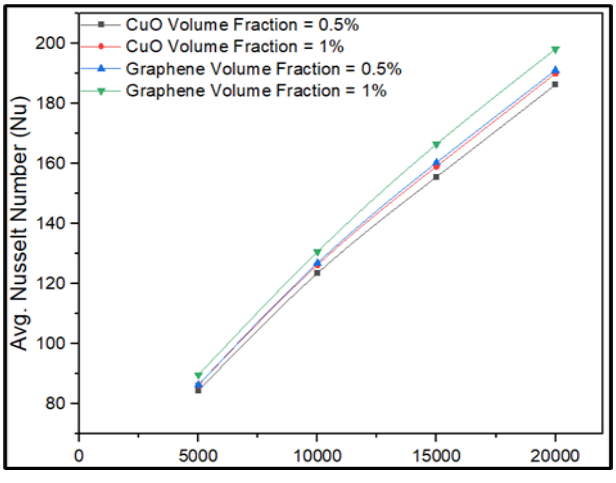


FIGURE 6. Average Nusselt number (Nu) vs. Reynolds number (Re) for CuO–water and Graphene–water nanofluids at 0.5% and 1.0% volume fractions

FRICTION FACTOR

The friction factor of nanofluid flow over the backward-facing step (BFS) channel was estimated by the relations of Eq. (4-8) with the average inlet and outlet temperatures taken as the reference temperature for the property estimation.

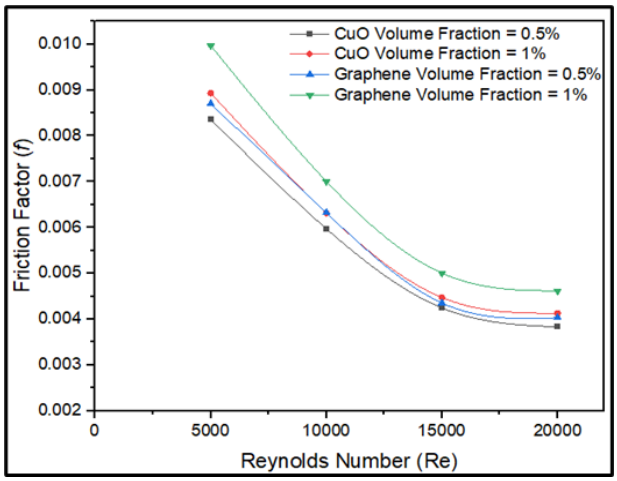


FIGURE 7. Variation of skin friction coefficient for CuO and graphene nanofluids at 0.5% and 1.0% volume concentrations with Reynolds number.

Figure 7 shows the direct comparison between CuO and graphene nanofluids at a concentration of 0.5% and 1%. It is demonstrated that for the same conditions, the friction factors of graphene nanofluids were always higher than that of CuO nanofluids, particularly at the low Reynolds numbers. This can be attributed to both the increased surface area of graphene and the increased contact of the graphene layer with the base fluid, hence increasing viscous drag. However, as *Re* increases the

discrepancy between the two types decreases, the results show the compromise among the optimized heat transfer and the flow resistance. Although thermal performance improves as the nanoparticle concentration increases (0.5-1.0%), the pressure drop increases simultaneously. To achieve good performance, there is a compromise between these two effects, especially for realistic heat exchanger applications.

As shown in Figure 8(a), the friction factor was increased with nanoparticle concentration. At the *Re* = 5000, the highest value was obtained by CuO nanofluid with 1.0% concentration, which is almost 35% greater than pure water. At the higher Reynolds numbers (*Re* = 15,000-20,000), this increase was smaller and the curves approached values of 0.00413-0.00447, thereby showing that at higher flow rates inertial forces are dominant over viscous resistance. For lower concentrations (0.1-0.3%) the increment was small, within 10-15% with respect to pure water.

Figure 8(b) shows the results for nanofluids based upon graphene. An increasing pattern of friction factor with increasing concentration was also noted. At *Re* = 5000, the optimum graphene nanofluid with 1.0% graphene content exhibited the highest value, which is more than 40% higher than that in pure water. For intermediate concentrations (0.3-0.5%), the increase was moderate (in the range of 20-25%). The values of friction factor decreased at higher Reynolds number indicating the lesser contribution of viscous force.

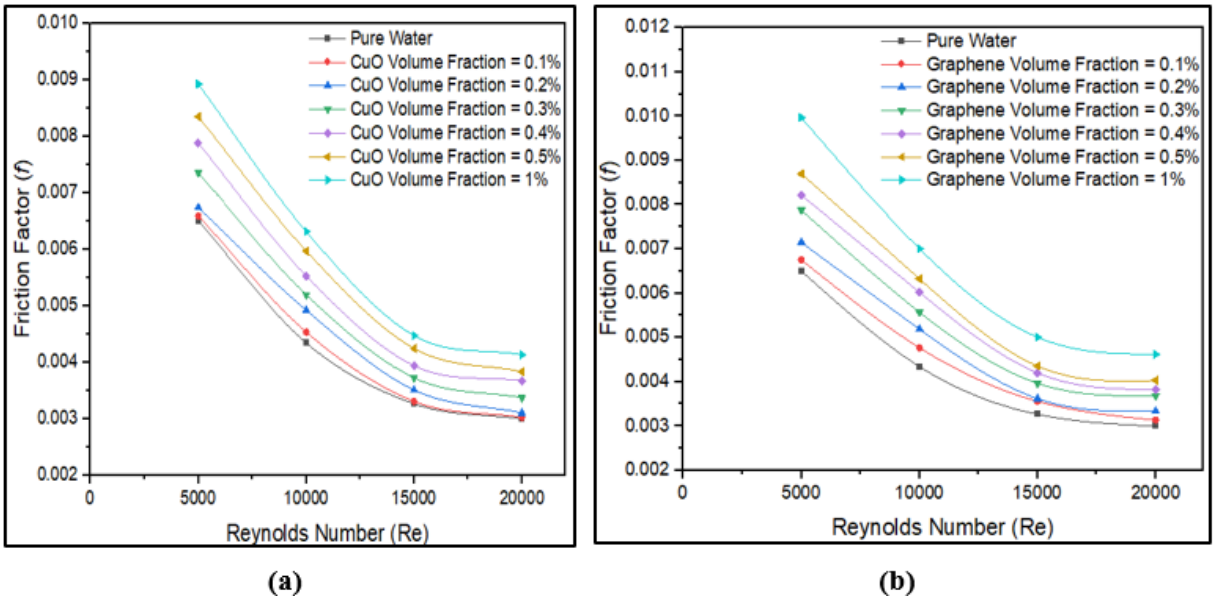


FIGURE 8. Variation of skin friction coefficient with Reynolds number (Re): (a) CuO–water nanofluids at different volume fractions (0.1–1.0%), (b) Graphene–water nanofluids at different volume fractions (0.1–1.0%).

PERFORMANCE EVALUATION CRITERIA

The application of nanofluids to backward facing step (BFS) channel improves heat transfer but at the same time increases flow resistance, especially with the increasing concentration of nanoparticles. To compare the effects of these two competing factors, the performance evaluation criterion (PEC) model was used. As can be seen from Eq. (20), PEC values higher than one mean that the gain obtained in heat transfer is larger than the penalty suffered due to higher friction. Higher PEC values therefore correspond to better thermal-hydraulic performance, and can help to find ideal nanoparticle concentrations for the optimal design of the systems.

Figure 9 shows the variation of PEC with *Re* for CuO- and graphene-water nanofluids. As shown in Figure 9(a), CuO nanofluids have maximum PEC of 1.58 at *Re* = 5000 and 1% volume fraction, which decreases gradually with *Re* because of less turbulence enhancement. Similarly, in Figure 9(b), even better performance was demonstrated for graphene nanofluids, as PEC equals 1.74 at 0.5% volume fraction and *Re* = 5000, which demonstrates the superior thermal conductivity and stability of graphene.

Figure 9(c) is a direct comparison between the CuO and graphene nanofluids at 0.5% and 1% concentrations. Graphene was always the better material than CuO, with higher PEC values in all *Re* ranges. As the nanoparticle loading increase, viscosity and friction increase while PEC

is marginally decreased at higher Re. *Nu* increased with nanoparticle loading but, the optimum fluid concentration for the best thermal-hydraulic efficiency was achieved with graphene nanofluids for BFS channel cooling application.

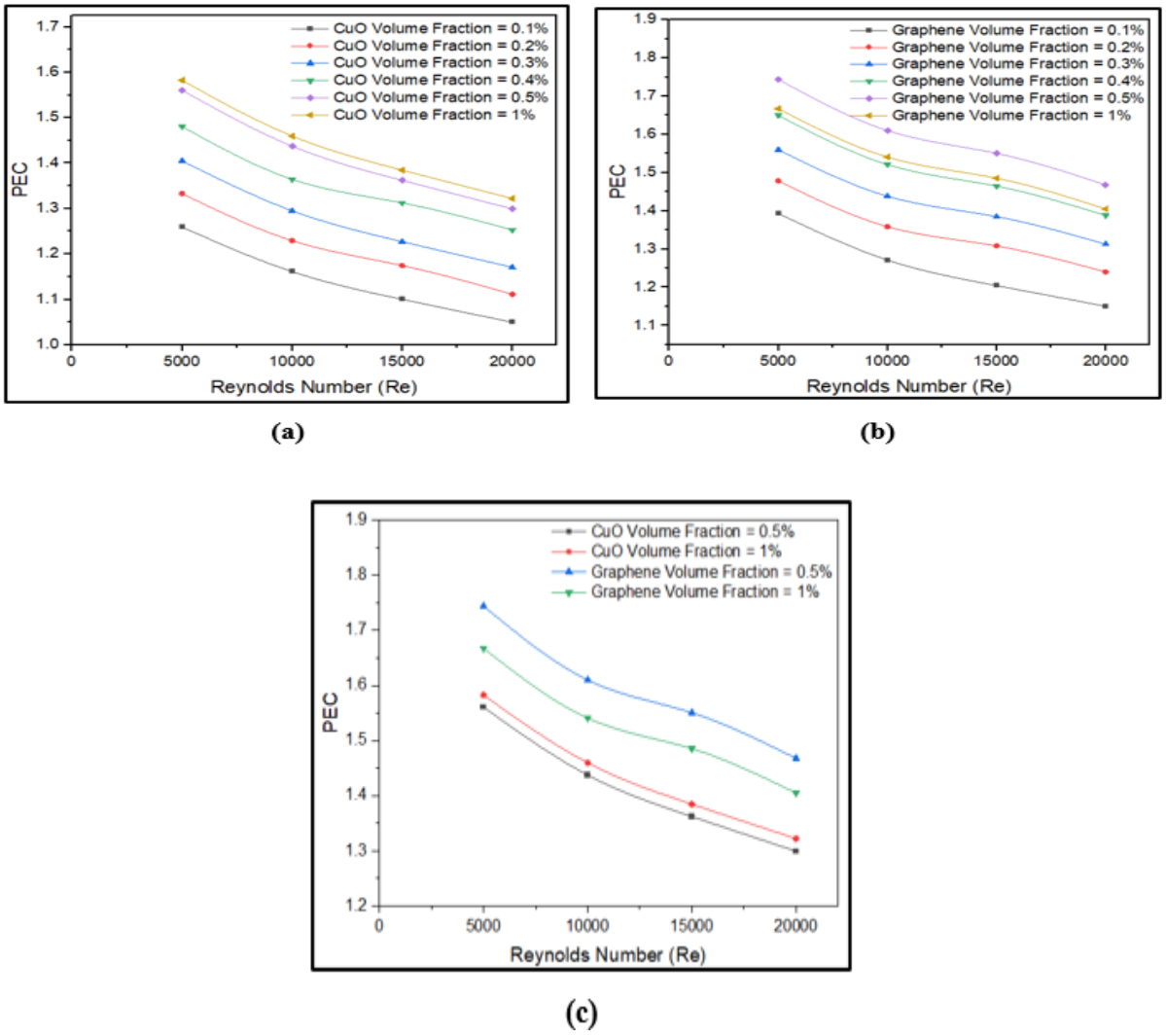


FIGURE 9. PEC variation with Reynolds number (Re): (a) CuO nanofluids, (b) Graphene nanofluids, (c) Comparison at 0.5% and 1.0% concentrations.

ALIGNMENT OF CUO AND GRAPHENE NANOFLUID STUDIES WITH PRESENT FINDINGS

As can be seen from Table 6, both CuO- and graphene-based nanofluids can generally improve heat transfer performance in all thermal systems. While most of the research focuses on BFS configurations, others examine geometries that are not BFS such as tubes, heat exchangers, annular ducts, and radiators, but all show significant enhancement over the taken reference point in terms of Nusselt number and convective performance. Improvements in CFD studies with CuO nanofluids have been found to be reasonably high (Nusselt number increase from 11% at low concentration (Talib et al. 2022) to more than 150-194% with combined obstacle/baffle (Rana et al. 2022; Bouazizi 2018), and they clearly indicate the significant effect of nanoparticle volume fraction and geometric adjustments on heat transfer.

Graphene nanofluids also show a lot of promise. Graphene oxide (GO-DW) enhanced Nusselt numbers by 11-14% at $Re = 7500$ (Karabulut & Alnak 2021), whereas highly crumpled few-layer graphene (HCFLG) and single-layer graphene nanofluids were reported to provide superior convective heat transfer coefficients and performance factors with high stability (Abdullah & Ibrahim 2017; Amiri, Arzani, et al. 2016). More recently, graphene nanoplatelets (GnP) have demonstrated a radical up-conversion rate of 1816% in radiators (Lik & Wei 2024), demonstrating their potential in future thermal systems.

In short, CuO nanofluids demonstrate heat transfer enhancements of 11% to 194%, whereas graphene-based nanofluids provide enhancements ranging from 11% to upwards of 1800%, depending on concentration, flow regime and system geometry. These results are in good agreement with the present study and verify the efficacy of CuO and graphene nanofluids on BFS heat transfer enhancement.

TABLE 6. Comparative Analysis of Heat Transfer Enhancements for CuO & Graphene nanofluids in BFS and Non-BFS Geometries

No.	Author(s)	Study Type	Geometry	Nanofluids	Findings
1	Selimefendigil & Öztop (2021)	Numerical	BFS + porous object	Hybrid (ND+Fe_3O_4/EG-water)	*Nu* ↑ 33% (geometry), 28.4% (NF); Opt. *Nu* = 2.037
2	Talib et al. (2022)	Experimental	BFS	CuO-EG & MgO-EG (0–5%)	CuO: *Nu* ↑ 11% at 5%, PEC = 1.5; MgO: PEC = 1.2
3	Mehrez & El Cafsi (2019)	Numerical	BFS + magnetic field	Al_2O_3–Cu/water (0.1–2%)	*Nu* ↑ with φ; reattachment ↓; strong Ha effect
4	Nath & Murugesan (2022)	Numerical	BFS + inclined MF	Cu–Al_2O_3/water	*Nu* ↑ 38% at 30°; buoyancy & Ha significant
5	Talib et al. (2022)	Experimental	Micro-BFS	CuO/water (0–0.04%)	Max PEC >1 at 3%; *Nu* ↑ with φ, Re; friction ↑
6	Pekmen Geridönmez & Öztop (2021)	Numerical	BFS + partial MF	CuO–Fe_3O_4/water (0.01–0.04%)	*Nu* max with sinusoidal inlet; weak at step center
7	Karabulut & Alnak (2021)	Numerical	BFS + chamfer	GO-DW (0.01–0.02%)	At *Re* = 7500: *Nu* ↑ 11.7% (0.01%), 14.3% (0.02%)
8	Pournaderi & Aram (2020)	Numerical	BFS	Six nanofluids: TiO_2, Fe_3O_4, CuO, Al_2O_3, ZnO, SiO_2	TiO_2 max Nu; CuO moderate; *Nu* & ΔP ↑ with φ (0.04), Re
9	Kherbeet et al. (2014)	Exp./Num.	Micro-BFS	SiO_2, Al_2O_3 (0–1%), CuO (5%)	SiO_2 highest Nu; Al_2O_3 higher friction; deviation ≤18.5%
10	Jourabian & Raeesi (2023)	Numerical	BFS + deflected wall	Cu, MWCNT-Fe_3O_4, hybrids	Max *Nu* ↑ 7% (Cu, Re=30215); deflection ↑ ANN 45%; PEC max 1.07
11	Amiri, Ahmadi, et al. (2016)	Experimental	BFS	HCFLG nanofluids	Significant *Nu* & h ↑ vs. DW; stability <2% sedimentation
12	Bouazizi (2018)	Numerical	BFS + square obstacle	CuO–water (0–15%)	*Nu* ↑ 194% (lower wall), 153% (upper wall); global *Nu* ↑ 108%
13	Abdullah & Ibrahim (2017)	Experimental	Tube (laminar)	GNPs–DI water (0.1–1 wt%)	Max *Nu* ratio = 1.45, PF = 1.24 (1 wt%, 6104 W/m²)
14	Syed (2025)	Exp./Num./ML	HX + nozzle insert	Water/graphene	PF ↑ 8.5–13.2%; nozzle boosts *h* via swirl flow
15	Mohammed et al. (2014)	Numerical	Vertical BFS (mixed conv.)	8 NFs (5%) incl. CuO	SiO_2 max Nu; buoyancy ↓ recirculation; skin friction ↓ with Re
16	Wahid et al. (2024)	Numerical	Shrinking disk	Graphene–Cu (1–2%)	2% Cu delayed BL separation 6%; *h* ↑ with slip/Soret effects
17	Ghanbari & Javaherdeh (2020)	Exp./Num.	Annular flow + baffles	0.2% nanoporous graphene	Avg. *Nu* ↑ 32%, ΔP ↑ 75%; efficiency ↑ 11.9% (3–7 baffles)
18	Hussein et al. (2019)	Numerical	Cubical cavity	Graphene–Pt (0–0.1%)	Avg. *Nu* ↑ with φ, Ri; max *Nu* when top wall moves −x
19	Lik & Wei (2024)	Numerical	Automotive radiator	GnP nanofluid	*Nu* ↑ up to 1816%; smaller tube/aspect ratio → better performance

continue...

...cont.

No.	Author(s)	Study Type	Geometry	Nanofluids	Findings
20	Fuller & Liu (2020)	Numerical	Microchannel entrance	CNTNf & GNPNf	GNPNf: *Nu* ↑ with φ; CNTNf: φ ↑ → heat transfer ↓
21	Rana et al. (2022)	Numerical	Micro-BFS + baffle	CuO/water (0–5%)	*Nu* ↑ 164% (Re=389, φ=5%); baffle height ↑ *Nu* & ΔP
22	Alawi et al. (2015)	Numerical	Vertical BFS + baffle	Al_2O_3, CuO, SiO_2, ZnO (1–4%)	SiO_2 highest Nu; CuO lower; *Nu* ↑ with φ, Re
23	Togun (2016)	Numerical	BFS + obstacles	CuO–water (1–4%)	Max *Nu* ↑ 22% (4.5 mm obstacle, Re=225); perf. ↑ 26–36% vs. water
24	(Mohamed et al. 2023)	Experimental	Double-pipe HX	CuO–water (0–0.4%)	Max h at φ=0.35%; *Nu* ↑ with φ, Re; friction ↑ with φ

The present data are compared with the earlier BFS and nanofluid studies and found that the heat transfer augmentation is found to be in the same trend as it increases with an increase in the value of Reynolds number, and also with the concentration of the nanoparticles, however, the friction loss is also increasing. The present study, however, provides new experimental evidence by direct comparison of the CuO-water and graphene-water nanofluids under the same trapezoidal corrugated BFS with obstacle. The results of the current study indicate that the graphene-water nanofluid has higher Nusselt number and PEC than CuO-water nanofluid which is not observed in previous studies mainly based on single nanofluids, numerical models or conventional BFS geometries. This proves that graphene is better suited for high performance BFS based thermal management and CuO is still a stable and moderate enhancing material.

CONCLUSION

The present work was conducted experimentally to study the thermal and hydraulic behavior of CuO-water nanofluid and graphene-water nanofluids in a backward-facing step (BFS) channel with trapezoidal corrugated walls and an obstacle at an expansion ratio of 2. The thermophysical properties of the nanofluids were measured and used to calculate Nusselt number (Nu), friction factor and performance evaluation criteria (PEC). Experiments were conducted in turbulent flow conditions in the range of Reynolds number (Re) from 5000-20,000 with the nanoparticle concentration of 0.1-1.0%.

The results confirmed that CuO and graphene nanofluids will improve convective heat transfer significantly higher than pure water. The average *Nu* increased monotonously with the volume fraction and the Reynolds number. At the lower concentrations (0.1%) the improvements were small since the viscosity effects could negate the thermal conductivity improvements, but at the higher concentrations (0.5-1.0%) the improvements in *Nu* were very large. A comparison between graphene nanofluids and CuO nanofluids showed that graphene nanofluids always had better performance than CuO nanofluids with higher *Nu* values in the whole *Re* range, mainly because the thermal conductivity and stability of graphene nanofluids were inherently better.

For both the nanofluids the friction factor was found to increase with an increase of nanoparticle concentration, and this increase was most notable in the low *Re* region. At a higher *Re* values, the effect of viscosity became less significant and the friction factor curves approached the same value. The graphene nanofluids with equivalent concentration had slightly higher friction factors compared to CuO, which indicates that graphene nanofluids had stronger interaction with the base fluid.

The PEC analysis showed that both nanofluids could offer good thermal-hydraulic performance with PEC > 1 for all cases. Also, maximum PEC values were found at low Reynolds numbers with moderate concentrations, indicating favorable trade-offs between the heat transfer enhancement and frictional losses. All graphene nanofluids showed PEC superior to CuO-based nanofluids with PEC values as high as 1.74 and 1.58, respectively, which reinforced their excellent properties for BFS-based cooling applications.

These results should be interpreted only in the light of the experimental conditions used in this work. The results are valid for CuO-water and graphene-water nanofluids flowing under turbulent flow condition in a trapezoidal corrugated BFS channel containing a single obstacle. Different thermal and hydraulic responses can be achieved by varying the type of nanoparticles, particle size, base fluid, addition of surfactant, geometry of obstacle, heat flux or the flow regime. Based on this, additional studies with varying channel arrangements, hybrid nanofluids, expanded operating ranges, and long-term

stability testing are recommended prior to scaling up to other applications for heat exchangers.

Overall, the results indicate that graphene nanofluids offer better thermal management than CuO nanofluids for BFS channels, but both types of nanofluids are found to have a measurable positive impact when used to improve the thermal performance of the BFS channel as compared to pure water. To further optimize the heat transfer performance of the advanced heat exchanger applications, hybrid nanofluids systems and extended geometrical alterations need to be investigated.

ACKNOWLEDGEMENT

None.

DECLARATION OF COMPETING INTEREST

None.

REFERENCES

Abdullah, NN & Ibrahim, HA. 2017. Experimental Study on Heat Transfer and Friction Factor Characteristics of Single Layer Graphene Based DI-water Nanofluid in a Circular Tube under Laminar Flow and Different Heat Fluxes as Boundary Conditions. *Journal of Engineering*. 23(5):106–122.

Abdulrazzaq, T, Togun, H, Goodarzi, M, Kazi, SN, Ariffin, MKA, Adam, NM & Hooman, K. 2020. Turbulent heat transfer and nanofluid flow in an annular cylinder with sudden reduction. *Journal of Thermal Analysis and Calorimetry*. 141(1):373–385.

Abu Talib, AR & Salman, S. 2023. Heat transfer and fluid flow analysis over the microscale backward-facing step using βGa2O3 nanoparticles. *Experimental Heat Transfer*. 36(3):358–375.

Ahmed, MA, Yusoff, MZ, Ng, KC & Shuaib, NH. 2015. Numerical investigations on the turbulent forced convection of nanofluids flow in a triangular-corrugated channel. *Case Studies in Thermal Engineering*. 6:212–225.

Ahmed, W, Zhan, Y, Zhang, H, Zhou, X, Shahid, M, Mudasar, F & Khan, QU. 2023. Preparation, applications, stability and improved thermal characteristics of sonochemically synthesized nanosuspension using varying heat exchangers, a Review: *Journal of Molecular Liquids*. 387.

Alawi, OA, Sidik, NAC & Mohammed, HA. 2015. Assisted and opposed mixed convective nanofluids flow over vertical backward facing step having a baffle. *Journal of Computational and Theoretical Nanoscience*. 12(9):2048–2061.

Amiri, A, Arzani, HK, Kazi, SN, Chew, BT & Badarudin, A. 2016. Backward-facing step heat transfer of the turbulent regime for functionalized graphene nanoplatelets based water-ethylene glycol nanofluids. *International Journal of Heat and Mass Transfer*. 97:538–546.

Amiri, A, Ahmadi, G, Shanbedi, M, Etemadi, M, Mohd Zubir, MN, Chew, BT & Kazi, SN. 2016. Heat transfer enhancement of water-based highly crumpled few-layer graphene nanofluids. *RSC Advances*. 6(107):105508–105527.

Asadi, A, Molana, M, Ghasemiasl, R, Armaghani, T, Pop, MI & Pour, MS. 2020. A new thermal conductivity model and two-phase mixed convection of CuO-water nanofluids in a novel I-shaped porous cavity heated by oriented triangular hot block. *Nanomaterials*. 10(11):1–19.

Azizi, M & Honarvar, B. 2021. Synthesis of highly stable nanofluids including polyvinyl alcohol-treated graphene oxide for improved heat dissipation in a tubular heat exchanger. *Journal of Thermal Analysis and Calorimetry*. 145(1):13–25.

Barai, RM, Kumar, D, Wankhade, A V., Sayed, AR & Junankar, AA. 2023. Experimental study of thermal characteristics of ZrO2/EG nanofluid for application of heat transfer. *Environmental Science and Pollution Research*. 30(10):25523–25531.

Belkassmi, Y, Gueraoui, K, El maimouni, L, Hassanain, N & Tata, O. 2021. Numerical Investigation and Optimization of a Flat Plate Solar Collector Operating with Cu/CuO/Al2O3–Water Nanofluids. *Transactions of Tianjin University*. 27(1):64–76.

Bindu, MV & Joselin Herbert, GM. 2022. Thermal conductivity and viscosity of Al2O3-ZnO-MWCNT-EG ternary nanofluid. *International Journal of Energy Research*. 46(12):17478–17496.

Bouazizi, L. 2018. Heat transfer enhancement in a backward-facing step with heated obstacle using nanofluid. *International Journal of Automotive and Mechanical Engineering*. 15(2):5195–5210.

Chakraborty, S, Shukla, D & Kumar Panigrahi, P. 2024. A review on coolant selection for thermal management of electronics and implementation of multiple-criteria decision-making approach. *Applied Thermal Engineering*. 245.

Chamkha, AJ & Selimefendigil, F. 2018. Forced convection of pulsating nanofluid flow over a backward facing step with various particle shapes. *Energies*. 11(11).

Dagdelen, OH & Ozceyhan, V. 2024. Experimental investigation of the effects of graphene nano particle added water fluid on heat transfer in a smooth tube with double inserts. *International Journal of Thermal Sciences*. 203.

Devendiran, DK & Amirtham, VA. 2016. A review

on preparation, characterization, properties and applications of nanofluids. *Renewable and Sustainable Energy Reviews*. 60:21–40.

Duda, P. 2023. Heat Transfer Coefficient Distribution—A Review of Calculation Methods. *Energies*. 16(9).

Fazeli, I, Sarmasti Emami, MR & Nazeri, MH. 2021. Comparing the effect of single and mixture surfactants on the improvement in stability and thermal conductivity of CuO nanofluid: an experimental study. *Journal of Thermal Analysis and Calorimetry*. 146(2):967–980.

Fuller, ME & Liu, JTC. 2020. Nanofluid flow and heat transfer of carbon nanotube and graphene platelette nanofluids in entrance region of microchannels. *Archives of Mechanics*. 72(4):355–379.

GaneshKumar, P, Sivalingam, VK, Vigneswaran, VS, Ramalingam, V, Seong Cheol, K & Vanaraj, R. 2024. Spray cooling for hydrogen vehicle, electronic devices, solar and building (low temperature) applications: A state-of-art review. *Renewable and Sustainable Energy Reviews*. 189.

Ghanbari, S & Javaherdeh, K. 2020. Investigation of applying nanoporous graphene non-Newtonian nanofluid on rheological properties and thermal performance in a turbulent annular flow with perforated baffles. *Journal of Thermal Analysis and Calorimetry*. 139(1):629–647.

Guo, X, Jasim, DJ, Alizadeh, A, Keivani, B, Nasajpour-Esfahani, N, Salahshour, S, Shamsborhan, M & Sabetvand, R. 2024. Investigating the effect of the number of layers of the atomic channel wall on Brownian displacement, thermophoresis, and thermal behavior of graphene/water nanofluid by molecular dynamics simulation. *Case Studies in Thermal Engineering*. 53.

Gupta, S & Subbarao, PMV. 2024. Empirical investigation of nanofluid performance in a microchannel heat sink for various attributes in low Reynolds number range. *International Journal of Heat and Fluid Flow*. 105.

Heidarshenas, A, Azizi, Z, Peyghambarzadeh, SM & Sayyahi, S. 2020. Experimental investigation of the particle size effect on heat transfer coefficient of Al2O3 nanofluid in a cylindrical microchannel heat sink. *Journal of Thermal Analysis and Calorimetry*. 141(2):957–967.

Hilo, AK, Abu Talib, AR, Acosta Iborra, A, Hameed Sultan, MT & Abdul Hamid, MF. 2020. Effect of corrugated wall combined with backward-facing step channel on fluid flow and heat transfer. *Energy*. 190.

Huang, P & Pan, M. 2021. Secondary heat transfer enhancement design of variable cross-section microchannels based on entransy analysis. *Renewable and Sustainable Energy Reviews*. 141.

Hussein, AK, Kolsi, L, Almeshaal, MA, Li, D, Ali, HM & Ahmed, IS. 2019. Mixed Convection in a Cubical Cavity With Active Lateral Walls and Filled With Hybrid Graphene-Platinum Nanofluid. *Journal of Thermal Science and Engineering Applications*. 11(4).

Ibrahim, NH, Cheplin, SNA, Shamsuddin, ZS & Aziz, ARA. 2025. Investigation of Power Generation from Air Conditioning Waste Heat Towards Sustainable Cooling Solution. *Jurnal Kejuruteraan*. 37(6):3055–3062.

Ishii, K, Ogiyama, T, Fumoto, K & Nishina, Y. 2024. Enhanced thermal conductivity of fluids by percolating high-concentration few-layer graphene. *Applied Physics Letters*. 125(2).

Ismael, LW. 2013. Experimental Investigation Ofthermal Conductivity Andpressuredropfor Water – Nanofluid Mixture. 13:570–586.

Jourabian, M & Raeesi, M. 2023. Turbulent forced convection flow of water-based nanofluids with temperature-dependent properties over backward-facing step channel with upwardly deflected downstream wall. *Numerical Heat Transfer; Part A: Applications*.

Karabulut, K & Alnak, DE. 2021. Investigation of Graphene Oxide-Distilled Water Nanofluids with Consideration of Heat Transfer and Flow Structure for Backward-Facing Step Flow. *Journal of Engineering Thermophysics*. 30(2):300–316.

Kherbeet, AS, Mohammed, HA, Munisamy, KM, Saidur, R, Salman, BH & Mahbubul, IM. 2014. Experimental and numerical study of nanofluid flow and heat transfer over microscale forward-facing step. *International Communications in Heat and Mass Transfer*. 57:319–329.

Kherbeet, AS, Mohammed, HA, Munisamy, KM & Salman, BH. 2015. Effect of base fluid on mixed convection nanofluid flow over microscale backward-facing step. *Journal of Computational and Theoretical Nanoscience*. 12(10):3076–3089.

Khouri, O, Goshayeshi, HR, Mousavi, SB, Hosseini Nami, S & Zeinali Heris, S. 2024. Heat Transfer Enhancement in Industrial Heat Exchangers Using Graphene Oxide Nanofluids. *ACS Omega*. 9(22):24025–24038.

Kiaee, FM, Bahrami, Z & Hormozi, F. 2020. Experimental investigation on the thermal performance and new correlation for thermal conductivity of aqueous copper oxide-doped MCM-41 nanofluids. *Journal of Thermal Analysis and Calorimetry*. 140(3):1443–1455.

Komeilibirjandi, A, Raffiee, AH, Maleki, A, Alhuyi Nazari, M & Safdari Shadloo, M. 2020. Thermal conductivity prediction of nanofluids containing CuO nanoparticles by using correlation and artificial neural network. *Journal of Thermal Analysis and Calorimetry*. 139(4):2679–2689.

Korpyś, M, Dzido, G, Al-Rashed, MH & Wójcik, J. 2020. Experimental and numerical study on heat transfer intensification in turbulent flow of CuO–water nanofluids in horizontal coil. *Chemical Engineering*

and Processing - Process Intensification. 153.

Lahmer, EB, Benhamou, J, Elouazzani, MA, Moussaoui, MA & Mezrhab, A. 2023. Heat transfer enhancement of a microchannel cooler with V-shaped partitions. *International Journal of Thermofluids*. 20.

Li, Z, He, YL, Tang, GH & Tao, WQ. 2007. Experimental and numerical studies of liquid flow and heat transfer in microtubes. *International Journal of Heat and Mass Transfer*. 50(17–18):3447–3460.

Lik, LTK & Wei, TT. 2024. Numerical Simulation of Graphene-Nanoplatelet Nanofluid Convection in Millimeter-Sized Automotive Radiator. *CFD Letters*. 16(6):32–52.

Magaji, IK, Ibrahim, A, Azeez, HL & Sopian, K. 2025. Comprehensive Review of Bio-Oil-Based Nanofluids as Cutting-Edge Heat Transfer Fluids with a Focus on Solar Thermal Systems. *Jurnal Kejuruteraan*. 37(5):2351–2376.

Magaji, IK, Ibrahim, A, Azeez, HL, Sopian, K & Ishak, MAA. 2025. Experimental Investigations of a Bio-oil-Based Binary Nanofluid as a Heat Transfer Fluid in Solar Thermal Systems. *Jurnal Kejuruteraan*. 37(8):3655–3672.

Manca, O, Nardini, S & Ricci, D. 2012. A numerical study of nanofluid forced convection in ribbed channels. *Applied Thermal Engineering*. 37:280–292.

Massey, JC, Langella, I & Swaminathan, N. 2019. A scaling law for the recirculation zone length behind a bluff body in reacting flows. *Journal of Fluid Mechanics*. 875:699–724.

Mayo, I, Virgilio, M, Cernat, BC & Arts, T. 2018. Measurement uncertainty in liquid crystal thermography applied to internal cooling research: Two practical examples. *Proceedings of the ASME Turbo Expo*. 5B-2018.

Mehrez, Z & El Cafsi, A. 2019. Forced convection magnetohydrodynamic Al2O3–Cu/water hybrid nanofluid flow over a backward-facing step. *Journal of Thermal Analysis and Calorimetry*. 135(2):1417–1427.

Milyani, AH, Al-Ebrahim, MA, Attar, ET, Abu-Hamdeh, NH, Mostafa, ME, Nusier, OK, Karimipour, A & Le, BN. 2023. Artificial intelligence optimization and experimental procedure for the effect of silicon dioxide particle size in silicon dioxide/deionized water nanofluid: Preparation, stability measurement and estimate the thermal conductivity of produced mixture. *Journal of Materials Research and Technology*. 26:2575–2586.

Ming, TZ, Zheng, Y, Liu, J, Liu, C, Liu, W & Huang, SY. 2010. Heat transfer enhancement by filling metal porous medium in central area of tubes. *Journal of the Energy Institute*. 83(1):17–24.

Mohamed, HA, Alhazmy, M, Mansour, F & Negeed, E-SR. 2023. Heat Transfer Enhancement Using CuO Nanofluid in a Double Pipe U-Bend Heat Exchanger. *Journal of Nanofluids*. 12(5):1260–1274.

Mohammadfam, Y & Zeinali Heris, S. 2023. An experimental study of the influence of Fe3O4, MWCNT-Fe3O4, and Fe3O4@MWCNT nanoparticles on the thermophysical characteristics and laminar convective heat transfer of nanofluids: A comparative study. *Surfaces and Interfaces*. 43.

Mohammed, HA & Salman, YK. 2007. Experimental investigation of mixed convection heat transfer for thermally developing flow in a horizontal circular cylinder. *Applied Thermal Engineering*. 27(8–9):1522–1533.

Mohammed, HA, Al-Aswadi, AA, Abu-Mulaweh, HI, Hussein, AK & Kanna, PR. 2014. Mixed convection over a backward-facing step in a vertical duct using nanofluids-buoyancy opposing case. *Journal of Computational and Theoretical Nanoscience*. 11(3):860–872.

Mubasyir, M. M., Abdullah, M. F., Ku Ahmad, K. Z., Othman, R. N. I. R. & Isahak, A. H. 2021. Energy Absorption AZ31B using Quenching in Nano Fluid. *Jurnal Kejuruteraan*. si4(2):29–37.

Nath, R & Murugesan, K. 2022. Double diffusive mixed convection in a Cu-Al2O3/water nanofluid filled backward facing step channel with inclined magnetic field and part heating load conditions. *Journal of Energy Storage*. 47.

Othman, Raja N. & Zainordin, MS. 2021. Thermal Conductivity Properties of Graphene Based Epoxy Nanocomposite. *Jurnal Kejuruteraan*. si4(2):59–64.

Ozturk, S, Hassan, YA & Ugaz, VM. 2013. Graphene-enhanced nanorefrigerants. *Nanoscale*. 5(2):541–547.

Pekmen Geridönmez, B & Öztop, HF. 2021. Effects of inlet velocity profiles of hybrid nanofluid flow on mixed convection through a backward facing step channel under partial magnetic field. *Chemical Physics*. 540.

Pournaderi, P & Aram, M. 2020. Numerical investigation of nanofluid flow and heat transfer over a backward-facing step. *Engineering and Applied Science Research*. 47(4):401–413.

Rahimi, A, Kasaeipoor, A, Malekshah, EH, Far, AS & Sepehr, M. 2018. Heat transfer intensification using CuO-water nanofluid in a finned capsule-shaped heat exchanger using lattice Boltzmann method. *Chemical Engineering and Processing - Process Intensification*. 127:17–27.

Rahimi Gheynani, A, Ali Akbari, O, Zarringhalam, M, Ahmadi Sheikh Shabani, G, Alnaqi, AA, Goodarzi, M & Toghraie, D. 2019. Investigating the effect of nanoparticles diameter on turbulent flow and heat transfer properties of non-Newtonian carboxymethyl cellulose/CuO fluid in a microtube. *International Journal of Numerical Methods for Heat and Fluid Flow*. 29(5):1699–1723.

Rana, S, Dura, HB, Bhattrai, S & Shrestha, R. 2022. Impact of baffle on forced convection heat transfer

of CuO/water nanofluid in a micro-scale backward facing step channel. *Journal of Thermal Engineering*. 8(3):310–322.

Ren, J, Jasim, DJ, Mohammad Sajadi, S, Nasajpour-Esfahani, N, Salahshour, S & Sabetvand, R. 2024. Investigating the initial pressure effect on Brownian displacement, thermophoresis, and thermal properties of graphene/ water nanofluid by molecular dynamics simulation. *Journal of Molecular Liquids*. 397.

Salameh, T, Alkasrawi, M, Olabi, AG, Makky, A Al & Abdelkareem, MA. 2023. Experimental and numerical analysis of heat transfer enhancement inside concentric counter flow tube heat exchanger using different nanofluids. *International Journal of Thermofluids*. 20.

Samad, S, Loh, KS, Yusoff, YN & Wong, WY. 2018. Morphological Studies on the Agglomeration of FeCo Supported Nitrogen-doped Reduced Graphene Oxide Catalyst Prepared at Varying Annealing Temperature. *Jurnal Kejuruteraan*. SI1(1):31–36.

Selimefendigil, F & Öztop, HF. 2021. Optimization of convective heat transfer performance for fluid flow over a facing step by using an elliptic porous object. *Case Studies in Thermal Engineering*. 27.

Shaik, AH, Chakraborty, S, Saboor, S, Kumar, KR, Majumdar, A, Rizwan, M, Arıcı, M & Chandan, MR. 2024. Cu-Graphene water-based hybrid nanofluids: synthesis, stability, thermophysical characterization, and figure of merit analysis. *Journal of Thermal Analysis and Calorimetry*. 149(7):2953–2968.

Siow, LT, Lee, JR, Ooi, EH & Lau, E Von. 2024. Application of graphene and graphene derivatives in cooling of photovoltaic (PV) solar panels: A review. *Renewable and Sustainable Energy Reviews*. 193.

Sohel Murshed, SM & Nieto de Castro, CA. 2017. A critical review of traditional and emerging techniques and fluids for electronics cooling. *Renewable and Sustainable Energy Reviews*. 78:821–833.

Syed, J. 2025. Enhancement of Heat Transfer Using Water/Graphene Nanofluid and the Impact of Passive Techniques—Experimental, Numerical, and ML Approaches. *Energies*. 18(1).

Taghreed, S, Kadom, Khairol, M, Mohd, A & Supeni, EE. 2025. Optimizing Heat Transfer : Corrugated Backward First Step Integration with Obstacles for Enhanced Performance Optimizing Heat Transfer : Corrugated Backward First Step Integration with Obstacles for Enhanced Performance. (April).

Talib, ARA, Salman, S, Zulkeple, MFM & Hilo, AK. 2022. Experimental Investigation of Nanofluid Turbulent Flow Over Microscale Backward-Facing Step. *Journal of Advanced Research in Fluid Mechanics and Thermal Sciences*. 99(2):119–134.

Thangapandian, E & Palanisamy, P. 2022. An experimental and numerical study to enhance the thermal characteristics of LA/CuO/Al2O3 nanocomposites as a phase change material for building cooling applications. *Polymer Composites*. 43(8):5426–5441.

Togun, H. 2016. Laminar CuO–water nano-fluid flow and heat transfer in a backward-facing step with and without obstacle. *Applied Nanoscience (Switzerland)*. 6(3):371–378.

Veeranna, Sridhara & Satapathy, N. 2011. Al2O3-based nanofluids: a review. *Nanoscale Research Letters*. 164(2):2011.

Verma, G, Saraj, CS, Mehlawat, K, Li, L & Li, W. 2025. Unveiling heat transfer mechanisms in rotational fluid systems: A teacup perspective. *Physics of Fluids*. 37(1).

Wahid, NS, Arifin, NM, Khashi'ie, NS & Pop, I. 2024. Unsteady axisymmetric hybrid graphene-copper nanofluid slip flow over a permeable radially shrinking disk with the Soret and Dufour effects. *International Journal of Heat and Fluid Flow*. 107.

Wang, W, Liu, G, Li, BW, Rao, ZH, Wang, H & Liao, SM. 2022. Momentum and heat transfer characteristics of three-dimensional CuO/water nanofluid flow in a horizontal annulus: influences of nanoparticle volume fraction and its mean diameter. *Journal of Thermal Analysis and Calorimetry*. 147(2):1757–1772.

Wang, Y-B, Yan, K-C, Wang, C-X, Wang, S-Y, Zhang, B-X, Yang, Y-R & Wang, X-D. 2024. Optimization study on fluid flow and heat transfer in a rectangular channel with cross-scale ribs for turbine blade internal cooling. *Physics of Fluids*. 36(12).

Xu, J, Shang, Z & Qing, S. 2025. Thermal Performance Analysis of Nanofluids for Heat Dissipation Based on Fluent. *Energies*. 18(1).

Yang, L, Ji, W, Mao, M & Huang, J nan. 2020. Dynamic stability, sedimentation, and time-dependent heat transfer characteristics of TiO2 and CNT nanofluids. *Journal of Thermal Analysis and Calorimetry*. 141(3):1183–1195.

Yanlin, J, Han, Y, Meng, F, Wu, Y & Jiani, LI. 2024. Optimization of enhanced heat transfer and flow resistance reduction in twisted petaloid helically coiled tube based on ZS-RSM and NSGA-II. *International Journal of Thermal Sciences*. 197.

Yousefi, S, Mahdavi, M, Soheil Mousavi Ajarostaghi, S & Sharifpur, M. 2023. Hydrothermal behavior of nanofluid flow in a microscale backward-facing step equipped with dimples and ribs; Lattice Boltzmann method approach. *Thermal Science and Engineering Progress*. 43.

Zolfalizadeh, M, Heris, SZ, Pourpasha, H, Mohammadpourfard, M & Meyer, JP. 2023. Experimental Investigation of the Effect of Graphene/ Water Nanofluid on the Heat Transfer of a Shell-and-Tube Heat Exchanger. *International Journal of Energy Research*. 2023.